ELSEVIER

Journal of Chromatography A, 917 (2001) 205–217

JOURNAL OF CHROMATOGRAPHY A

www.elsevier.com/locate/chroma

Miniature radio-frequency mobility analyzer as a gas chromatographic detector for oxygen-containing volatile organic compounds, pheromones and other insect attractants

G.A. Eiceman[a,*], B. Tadjikov[a], E. Krylov[a], E.G. Nazarov[a], R.A. Miller[b], J. Westbrook[c], P. Funk[d]

[a]*Department of Chemistry and Biochemistry, New Mexico State University, Box 30001-Dept. 3C, Las Cruces, NM 88003-0001, USA*
[b]*Charles Stark Draper Laboratory, Cambridge, MA, USA*
[c]*US Department of Agriculture, Agricultural Research Service, Areawide Pest Management Research, College Station, TX 77845, USA*
[d]*US Department of Agriculture, Agricultural Research Services, SW Cotton Ginning Research Laboratory, Las Cruces, NM 88047, USA*

Received 28 November 2000; received in revised form 13 February 2001; accepted 13 February 2001

Abstract

A high electric field, radio-frequency ion mobility spectrometry (RF-IMS) analyzer was used as a small detector in gas chromatographic separations of mixtures of volatile organic compounds including alcohols, aldehydes, esters, ethers, pheromones, and other chemical attractants for insects. The detector was equipped with a 2 mCi ^{63}Ni ion source and the drift region for ion characterization was 5 mm wide, 15 mm long and 0.5 mm high. The rate of scanning for the compensation voltages was 60 V s^{-1} and permitted four to six scans to be obtained across a capillary chromatographic elution profile for each component. The RF-IMS scans were characteristic of a compound and provided a second dimension of chemical identity to chromatographic retention adding specificity in instances of co-elution. Limits of detection were 1.6–55$\times 10^{-11}$ g with an average detection limit for all chemicals of 9.4$\times 10^{-11}$ g. Response to mass was linear from 2–50$\times 10^{-10}$ g with an average sensitivity of 4 pA ng^{-1}. Separations of pheromones and chemical attractants for insects illustrated the distinct patterns obtained from gas chromatography with RF-IMS scans in real time and suggest an analytical utility of the RF-IMS as a small, advanced detector for on-site gas chromatographs.

Keywords: Radio-frequency ion mobility spectrometry; Detection, GC; Volatile organic compounds; Pheromones; Aldehydes; Ethers; Esters; Alcohols

1. Introduction

Relatively robust on-site gas chromatographs have received considerable attention in the past decade with emphasis on developing miniature, portable, or high-speed instruments [1–4]. One of the motivations in creating such gas chromatography (GC) analyzers is an interest in making measurements in-situ at industrial or environmental venues. Portable gas chromatographs differ from process analyzers in size, utilities, weight and resolving power. Certain components or facets of high speed

*Corresponding author. Tel.: +1-505-646-2146; fax: +1-505-6466094.
E-mail address: geiceman@nmsu.edu (G.A. Eiceman).

0021-9673/01/$ – see front matter
PII: S0021-9673(01)00656-2

or portable gas chromatographs have reached an advanced stage of refinement and include columns [5–7], injectors [8] and temperature control of the column [9]. In contrast, detectors for portable gas chromatographs have limitations principally vis-a-vis detection limits or sensitivity. In addition, common GC detectors such as thermal conductivity detectors and photoionization detectors lack a second dimension of chemical information that augments specificity from chromatographic retention data. This is evident for laboratory based instruments with the gas chromatography–mass spectrometry where mass spectra have dramatically increased the value of analytical separations. Unfortunately, such orthogonal information is not available routinely from those detectors which are best suited for small, fieldable instruments. Fieldable mass spectrometers are now commercially available as robust GC–MS instruments [10] and are limited largely by their high cost.

Mobility spectrometers [11] have been described as detectors for gas chromatographs from early in the development of ion mobility spectrometry (IMS) and the first successful use of IMS detectors with capillary chromatography occurred in 1982 [12]. High-speed response and low memory effects were attained by creating low residence time of sample vapors in the ion source and by preventing sample neutrals from diffusing into the drift region. A secondary benefit from this advance was that the gas phase ion chemistry inside an IMS system became highly reproducible and provided the foundation to glean chemical class information from mobility spectra [13]. Thus, mobility spectrometers, as ionization detectors for GC, exhibit functional parallels to mass spectrometers, except all processes in IMS occur at ambient pressure making vacuum systems unnecessary. The concept of a gas chromatograph with an ion mobility detector eventually was recognized as economical and sensible when utilities, size, weight and cost became practical considerations. This can be seen in the volatile organic analyzer or VOA (a GC–IMS instrument) which is planned for air quality monitoring on-board the international space station [14]. Others have recognized the usefulness of combined GC–IMS methods for chemical agent monitoring [15], in explosives detection [16] and for some environmental uses of IMS [17]. A successful field instrument should include both a small injector/column and a small detector (i.e. small mobility spectrometer) and despite advances of the past decade, conventional IMS drift tubes are still comparatively large and expensive or suffer from losses in detection limits when made small [18–20].

In 2000, a micro-machined drift tube was described and was based upon a recently proven method of ion filtering using high frequency high voltage waveforms [21]. This new method of ion characterization by high field asymmetric waveforms is under active development [22–27] following a first practical demonstration [22]; a complete assessment of this technique is progressing. In the method of high field radio frequency mobility, ions are characterized using differences between ion mobilities under oscillating high and low electric fields (see Section 2). The fields are applied perpendicular to ion transport favoring a planar drift tube configuration which can be fabricated inexpensively with small dimensions [21]. Also, electronics can be made small (as shown in Fig. 1) and total power is estimated as 6–10 W (unheated), a level that is suitable for field instrumentation. Previously, the scan rates of the high field mobility analyzers was regarded as too slow to monitor the effluent of a fast capillary gas chromatograph. However, the small size of the miniature mobility analyzer allows ion residence times of <1 ms and the scan time for an entire spectrum can be less than 1 s. This makes the speed of ion characterization comparable to that of a modern quadrupole mass spectrometer which like the RF-IMS system operates as an ion filter in vacuum. Consequently, the opportunity exists to provide a gas chromatographic detector where retention time is supplemented with orthogonal information, here measurements associated with mobilities of ions in asymmetric electric fields.

In this report, a first description is given for a miniature RF-IMS detector where possibilities exist for portable GC instrumentation without the complications of weight, powers, and size of conventional IMS drift tubes. The goal for this study is to obtain a first measure of performance of a small RF-IMS system as a GC detector including the determination of limits of determination (LODs) and response curves for a range of chemicals. In addition, analysis will be provided for the usefulness of RF-IMS scans for a range of chemicals to add selectivity to

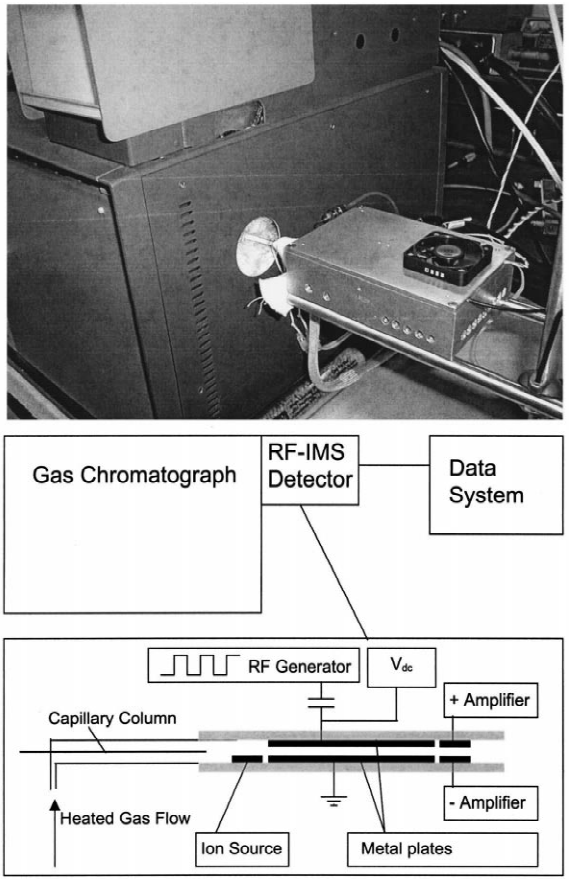

Fig. 1. Photograph of detector with insets of the detector design.

chromatographic separations. While the initial application of this sensor is to detect pheromones and other insect attractants, the eventual goal is to provide an advanced detector for field GC instruments. Consequently, emphasis was given to response toward oxygen-containing volatile organic compounds.

2. Principles of high electric field RF-IMS

In high electric field radio frequency mobility measurements, a carrier gas is used to carry ions through the analyzer where a RF electric field, $E(t)$, is applied to parallel plates as shown in Fig. 1. The amplitude of the RF field is asymmetric (where E_{max}~20000 V cm^{-1} and E_{min}~5000 V cm^{-1}) and this field causes ions to oscillate in a direction transverse to the direction of flow of the carrier gas. Ion velocities in the transverse or perpendicular direction under high field conditions will differ from those under low fields with each described by Eq. (1):

$$v_{\perp}(t) = K(E) \cdot E(t) \quad (1)$$

where terms are: $v_{\perp}$, instantaneous ion velocity in perpendicular motion; $K(E)$, field dependent mobility; and $E(t)$, instantaneous electric field strength. Since displacement of the ion under high fields is greater than that for low fields, the ion is drawn toward one plate by a net amount Δh for each period. The average value of $\pm\Delta h$ for an ion species is determined by the waveform and frequency of the RF field and difference between the field dependent mobility values $K(E)$. The total displacement of the ion in space is $n\Delta h$ as governed by the number of RF periods (n). Ions eventually collide with the drift tube wall, are neutralized or annihilated and are removed from the drift region in the gas flow.

An ion can be passed through the drift region, in the RF fields and without striking the walls, to the detector by applying a low-voltage d.c. field to the ion plates in opposition to the net RF-induced transverse motion of the ion. Moreover, a sweep of compensation voltage will provide a measure of all the ions in the analyzer resulting in a RF high-field mobility scan. Thus, both ion characterization and ion separation can be understood as a difference in mobility [i.e. $K(E_H) - K(E_L)$] where $K(E_H)$ is the mobility at the higher field and $K(E_L)$ is the mobility at lower field. In traditional low field IMS, ion mobilities are reasonably well-described through the Mason–Schamp equation [28] and reduced mobility constants (K_o) are related to reduced mass and cross-section areas for ion–molecule collisions where ion mobilities are independent of electric field. In contrast, the relationship between molecular structure and the coefficient of mobility in the high electric field, $K(E)$, for multi-atomic organic ions is barely described. Moreover, relationships between conventional terms of mass and collisional cross section are unknown at present. One link between ion behavior and conventional mobility constants is shown in Eq.

(2) where $K(E)$ is the ion mobility for any field, K_o is the mobility constant at low field, E is the electric field strength and α is the slope of the graph of $K(E)$ versus E [22]:

$$K(E) = K_o[1 + \alpha(E)] \quad (2)$$

The term, α, can be positive or negative for an ion regardless of ion polarity and describes the slope and direction of the plot of $K(E)$ versus E. In short, an RF IMS provides details on the composition of ions present in the ionization chamber, here a β source. In this regard, the detector should have a quantitative response comparable to atmospheric pressure chemical ionization mass spectrometry with the size of a small electron-capture detection (ECD) system. However, unlike an ECD, this detector will operate with positive and negative ions and provide an RF-mobility scan with content about ion composition of a sample.

3. Experimental

3.1. Instrumentation

A model 5710 gas chromatograph (Hewlett-Packard, Avondale, PA, USA) was equipped with a HP split–splitless injector, 25-m SP 2300 capillary column (Supelco, Bellefonte, PA, USA), and an RF-IMS analyzer as a detector. This analyzer has been described in detail [21,29] and was fabricated in a planar manner using rectangular metal electrodes on the surface of two planes that formed the body of the drift tube. The body of drift tube was 5 mm wide, 15 mm long with a 0.5-mm spacing between planes; however, the dimensions of the metal electrodes, where flow was constrained and where ions were separated, were 5 mm wide by 10 mm long. Air was provided to the drift tube at 2–3 l min^{-1} and was provided from a model 737 Addco Pure Air generator (Miami, FL, USA) and further purified over a 5-Å molecular sieve bed (0.6 m long by 10 cm diameter). The drift tube was placed against one side of an aluminum box which also included the amplifier and RF circuit as shown in Fig. 1. A 10-cm section of capillary column was passed through a heated tube to the mobility analyzer. The GC carrier gas was nitrogen (99.99%) scrubbed over a molecular sieve bed. Pressure on the splitless injector was 10 p.s.i.g and the split ratio was 200:1.

The compensation voltage was scanned from −18 to +4 V_{dc} at 60 V s^{-1} and each scan was made in ~1 s. Thus, several RF scans could be obtained over the elution profile of a peak in a chromatogram where peak widths were from ~5 to 10 s each at baseline. The asymmetric waveform had a high voltage of 1.0 kV (20 kV cm^{-1}) and a low voltage of −250 V (−4.167 kV cm^{-1}). The frequency was 1.25 MHz and the high frequency had a 20% duty cycle. The amplifier exhibited linear response time and bandwidth of 7 ms and 140 Hz, respectively. Signal was processed using a National Instruments board (model 6024E) to digitize and store the scans and specialized software to display the results as spectra, topographic plots and graphs of ion intensity versus time. The ion source was a small ^{63}Ni foil with total activity of 2 mCi. However, a substantial amount of ion flux from the foil was lost by the geometry of the ionization region and the estimated effective activity is 2 mCi.

3.2. Chemicals and reagents

Stock solutions of alcohols, aldehydes, ethers and esters were obtained in reagent grade from various commercial sources. A pheromone, Grandlure, was obtained from Hercon Environmental Corp. (Emigsville, PA, USA) and is a mixture of four chemicals including ±(*Z*)-2-isopropenyl-1-methylcyclobutylethanol, (*Z*)-3,3-dimethylcylcohexyledeneethanol, (*Z*)-3,3-dimethylcylcohexylideneacetaldehyde, (*E*)-3,3-dimethylcylcohexylideneacetaldehyde in the ratio of 30:40:15:15 (v/v), respectively. An insect attractant, Mix M, was made from phenylacetaldehyde, limonene, 2-phenylethanol, methyl salicylate, methyl-2-methoxybenzoate in gram amounts of 5.77, 5.89, 5.51, 2.49, and 4.88, respectively.

3.3. Procedures

3.3.1. General

The procedures for injecting a sample were standard and involved split injection with a ratio of 1:200. The oven program for standard solutions was 40°C for 4 min then 40–260°C at 16°C min^{-1}. Exceptions included alcohols which were programmed at a rate of 8°C min^{-1} and aldehydes

where the starting temperature was 60°C. The Grand Lure and Mix M were separated with the program from 70 to 220°C at 8°C min^{-1} with a final time of 8 min.

3.3.2. Quantitative

Stock solutions of the various compounds were made using methylene chloride solvent in the 10–100 ppm range per compound. Stock solutions were made as mixtures by chemical class. These were later made into working concentrations by serial dilution of the stock solutions from 100:1 to 3200:1. All solutions were analyzed in triplicate.

4. Results and discussion

4.1. RF-mobility analyzer as detector in gas chromatography of oxygen-containing volatile organic compounds

The separation of aldehydes is shown in Fig. 2 as a chromatogram (right frame) and as the associated two-dimensional plot (left frame) for ion intensity versus compensation voltage from the RF-mobility scans of GC effluent. The axis for detector response in the chromatogram is the sum of peak intensity for the product ions created in the RF-IMS analyzer and does not include the intensity of either the reactant ions or the solvent peak for methylene chloride (present at compensation voltages of −10 and +2 V_{dc}, respectively). The separation of a homologous series of aldehydes (propanal to nonanal) with a linear temperature program shows a regular interval in retention on a slightly non-polar phase starting after an isothermal period at 40°C. The compressed retention intervals from 0 to 200 s suggested that initial temperature was slightly high for complete resolution of the smallest aldehydes. Since baseline separation was attained for most components the temperature program was used with the lower initial temperature of 40°C instead of 60°C. The peak shape is adequate with slight tailing and asymmetry factors of 1.5–3.6. The height equivalent of theoretical plates (H) ranged from 0.09 to 1.1 mm. The column and chromatographic conditions provided suitable separations though not optimum and emphasis was given to evaluating the RF-IMS detector. Retention times and other chromatographic measures are summarized in Table 1.

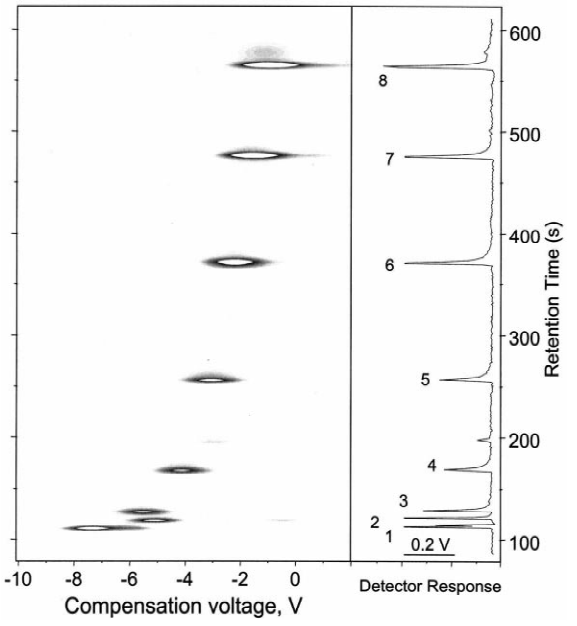

Fig. 2. Results from GC–RF-IMS separation of mixture of aldehydes with chromatograms (right frame) and two-dimensional plots of RF-IMS scans (left frame). Peak identities are given in Table 1.

The value of RF-IMS scans can be seen in the left frame of Fig. 2 where the two-dimensional (2D) information is shown from the GC separation. The patterns evident in this frame illustrate the orthogonal information available in scans with the miniature RF-IMS analyzer. The plots demonstrate that each chromatographic peak can be associated with RF-IMS scans throughout the elution profile and that the scans are distinctive or characteristic. Details on the structure of these scans can be seen in Fig. 3 as plots of ion intensity versus compensation voltage. These spectra were selected from the maxima of the chromatographic peaks (i.e. high abundance). The RF-IMS scans for these compounds are shown in Fig. 3 and illustrate the chemical information available from this miniature detector. The RF-IMS scans show near constant peak widths (full width half-maximum or FWHM of ~1 V_{dc}) for each compound. Peak widths here were broader than prior RF-IMS studies in order to improve sensitivity. The RF-IMS scans also yielded peak maxima which ranged from −7.22 to −0.85 V. and showed a pattern of decreasing V_{dc} with increased molecular mass or ion size.

Table 1
Results from separation of oxygen containing using GC with miniature RF-mobility analyzer

Compound	Retention time (s)	*H* (mm)	Peak maximum from RF-mobility scan V_{dc}	LOD (pg, $S/N=2$)	Assymetry factor, γ
Aldehydes (60°C for 4 min then 40–260°C at 16°C min^{-1})					
(1) Propanal	112	–	−7.22; −2.05	26	1.5
(2) 2-Methylpropanal	121	0.48	−5.02; −0.35	34	1.5
(3) Butanal	128	1.1	−5.4; −0.86	57	1.5
(4) Pentanal	167	0.82	−4.03; −0.13	92	3.2
(5) Hexanal	256	0.52	−2.93; 0.26	105	3.6
(6) Heptanal	369	0.21	−2.12; 0.65	79	3.4
(7) Octanal	474	0.10	−1.53; 0.87	61	2.5
(8) Nonanal	563	0.09	−0.85; 1.2	49	2.4
Ethers (40°C for 4 min then 40–260°C at 16°C min^{-1})					
(1) *tert.*-Butyl methyl ether	135	0.39	−7.22; 0.92	16	1.5
(2) Isopropyl ether	149	0.46	−2.27; 0.92	25	1.7
(3) Butyl methyl ether	162	0.39	−3.32; 0.31	31	3
(4) Isobutyl vinyl ether	187	0.39	−7.03; −3; 0.97	30	1.3
(5) *tert.*-Amyl methyl ether	205	0.43	−5.74; 1.03	21	1.3
(6) Propyl ether	216	0.49	−2.51; 0.58	29	2.4
(7) Butyl ethyl ether	226	0.45	−2.49; 0.59	35	2
(8) Butyl ether	450	0.09	−0.86; 1.03	27	1.6
(9) Pentyl ether	621	0.05	0.22	25	1.4
(10) Hexyl ether	763	0.21	0.69	60	1.3
Esters (40°C for 4 min then 40–260°C at 16°C min^{-1})					
(1) Methyl acetate	127	0.44	−6.1	–	–
(2) Ethyl acetate	159	0.28	−4.47; 0.04	22	6
(3) Isopropyl acetate	193	0.19	−6.73; −2.82; 0.65	44	2.4
(4) Methyl isobutyrate	217	1.2	−2.71; 0.7	51	2
(5) *tert.*-Butyl acetate	239	0.24	−7.33; 1.2	48	1.6
(6) Methyl trimethyl acetate	262	0.33	−1.12; 1.31	19	1.7
(7) Methyl isovalerate	329	0.21	−2.0; 1.14	40	1.8
(8) *n*-Butyl acetate	377	0.20	−2.27;	85	4.6
(9) Methyl isocaproate	460	0.16	−1.23; 1.2	30	1.83
(10) 2-Ethoxyethyl acetate	479	0.08	−1.49	40	–
(11) Methyl hexanoate	494	0.14	−1.45; 1.31	45	3
(12) Methyl heptanoate	582	0.08	−0.8; 1.5	45	3
(13) Methyl octanoate	660	0.08	−0.35; 1.67	50	2.6
Alcohols (40°C for 4 min then 40–260°C at 8°C min^{-1})					
(1) Ethanol	108	1.2	−7.72; −4.31	100	2.8
(2) 2-Propanol	114	1.8	−7.55; −1.5	79	2.8
(3) *tert.*-Butanol	120	1.6	−7.28; 0.48	129	2.5
(4) 1-Propanol	131	1.0	−7.44; −1.67	204	4.3
(5) 2-Butanol	148	0.63	−7.5; −0.4	213	4.2
(6) 2-Methyl-1-propanol	163	1.3	−7.53; −0.48	122	5
(7) 1-Butanol	193	2.4	−7.28; −0.3	484	7.2
(8) 3-Methyl-1-butanol	278	0.93	−5.57; −2.82; 0.54	340	3.6
(9) 4-Methyl-2-pentanol	312	0.49	−4.2; 0.92	231	3
(10) 2-Butoxyethanol	554	0.83	−2.1; 0.65	541	11

These scans are the first ever shown for a systematic evaluation of a homologous series and the principles that underlie the mechanism of ion characterization and separation in RF-IMS are incomplete. Thus, these findings cannot be rationalized for V_{dc} versus ion structure since models to not exist for such

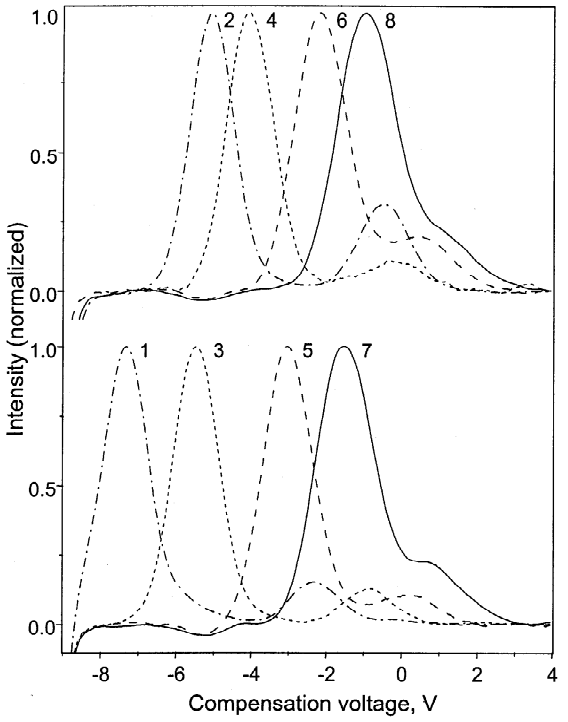

Fig. 3. Plots of detector current versus compensation voltage from RF-IMS scans for aldehydes. Compounds are (1) propanal, (2) 2-methylpropanal, (3) butanal, (4) pentanal, (5) hexanal, (6) heptanal, (7) octanal and (8) nonanal. Numbers for chemicals are the same as those in Fig. 2.

analysis. The scans are restricted here to use as analytical information only without explanation of fundamentals of response. This topic is under active development in several laboratories at this writing.

The gas phase chemistry that underlies the RF-IMS however is well-known and is based upon atmospheric pressure chemical ionization with hydrated protons as reactant ions. The peak for the reactant ions is not shown on the 2D plots of Fig. 2 and appeared at V_{dc} of -9 to -10. The intensity for the reactant ion peak was $10\times$ the intensity of the product ion peaks. As the concentration of the sample vapors increased in each elution profile, the reactant ion peak intensity declined as would be expected for the gas phase chemistry of ^{63}Ni beta sources. The reactions are based upon proton transfer reactions and the product ions in Fig. 3 may be reasonably anticipated to be species such as a protonated monomer (MH^+) or a proton bound dimer (M_2H^+). A common pattern in mobility spectra from traditional mobility spectrometers is the dependence of the ratio of peak intensities for MH^+ / M_2H^+ upon sample concentrations. In the spectra of Fig. 3, there is no apparent dependence on concentration suggesting that ions are protonated monomers only; however, any ion identity postulated here should be regarded as speculative pending IMS–MS identifications. The analytical importance of these plots are that the miniature RF-IMS analyzer provides a second dimension of information that is not available from simple ionization or thermal conductivity detectors. Barely visible on the 2D plot of Fig. 2 are second peaks in RF-IMS scans for some chemicals. These peaks were concentration dependent, were more pronounced for other compound classes and are discussed for ethers.

Results from GC–RF-IMS characterization of mixtures of ethers are shown in Figs. 4 and 5 and RF-IMS scans can be compared directly to those for aldehydes presented above. Quantitative details on both the GC separations and the peak shape or maxima from RF-IMS scans are summarized in Table 1. Baseline resolution was attained with the

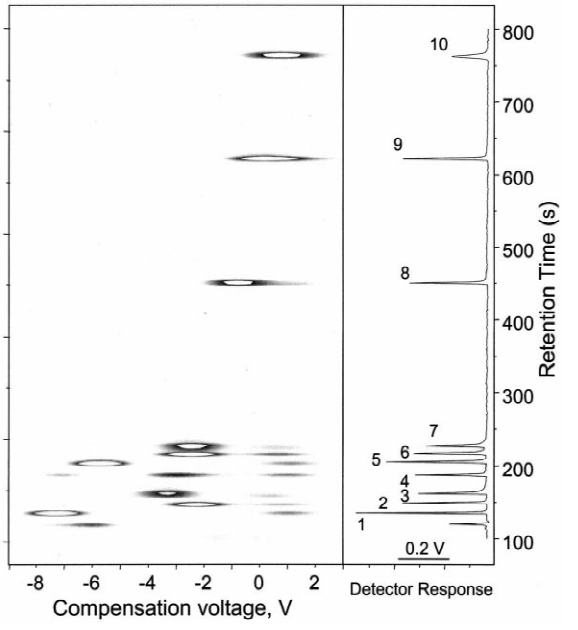

Fig. 4. Results from GC–RF-IMS separation of mixture of ethers with chromatograms (right frame) and two-dimensional plots of RF-IMS scans (left frame). Peak identities are given in Table 1.

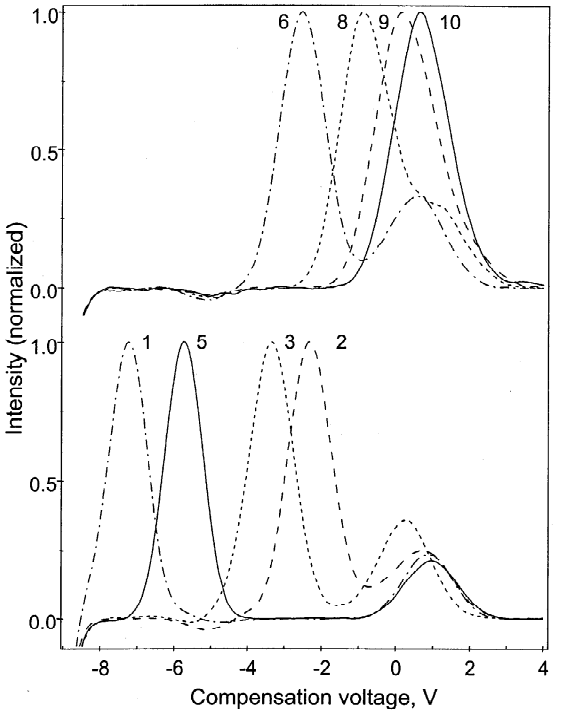

Fig. 5. Plots of detector current versus compensation voltage from RF-IMS scans for ethers. Compounds are (1) *tert*.-butyl methyl ether, (2) isopropyl ether, (3) butyl methyl ether, (5) *tert*.-amyl methyl ether, (6) propyl ether, (8) butyl ether, (9) pentyl ether, and (10) hexyl ether. Numbers for chemicals are the same as those in Fig. 4.

more volatile compounds with the lower initial temperature though consequently the retention time scale was increased to 800 s. The asymmetry factors for ethers were improved over that for aldehydes. The separations and peak shape were adequate for this first demonstration of RF-IMS analyzers as GC detectors. Peak maxima from the RF-IMS scans were distributed between V_{dc} values of -8 to $+1$ V as seen in Fig. 5. A feature seen distinctly in these RF-IMS scans is the presence of an additional low intensity peak at V_{dc} values of 0 to $+1.5$ V in some of the small ethers (Fig. 5, bottom frame). These peaks increased with high vapor concentration levels and confirmation of peak identities is pending IMS–MS studies now underway. Still, this second peak (visible in peaks 1–7 of Fig. 4, right frame) are consistent with cluster ions such as proton bound dimers. There are some other ethers that have the same or very similar V_{dc} values as those for aldehydes; however, no pair or match of compounds have the same pair of V_{dc} values when the second peak was included (see Table 1).

Results from GC–RF-IMS characterization of a mixture of esters are shown in Figs. 6 and 7 where the chromatographic separation and the orthogonal information provided by the RF-IMS scans are shown. As with previous results described above, the chromatographic efficiency for esters ranged from HETP values of 0.08–1.2 mm and baseline separations were obtained throughout. The low initial temperature cause retention of larger esters past 600 s and the retention time scale in Fig. 6 was extended to 800 s. The RF-IMS scans in Fig. 7 show a progression of peak maxima with increase in molecular mass and heavier compounds were displaced from -8 V toward $+1$ V. Notable amongst these results is the apparent aberration for *tert*.-butyl acetate where the peak from the RF-IMS scan was located at -7.33 V_{dc} rather than the anticipated -4 to -2 V_{dc}. In traditional IMS, *tert*.-butyl acetate is known to undergo thermal decomposition to frag-

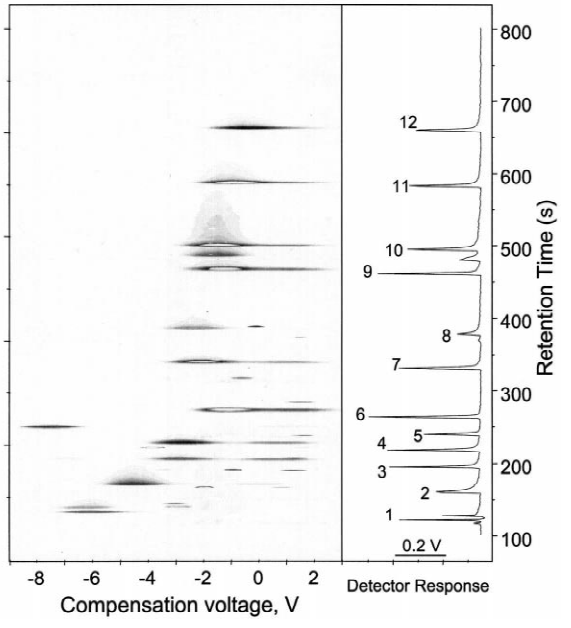

Fig. 6. Results from GC–RF-IMS separation of mixture of esters with chromatograms (right frame) and two-dimensional plots of RF-IMS scans (left frame). Peak identities are given in Table 1.

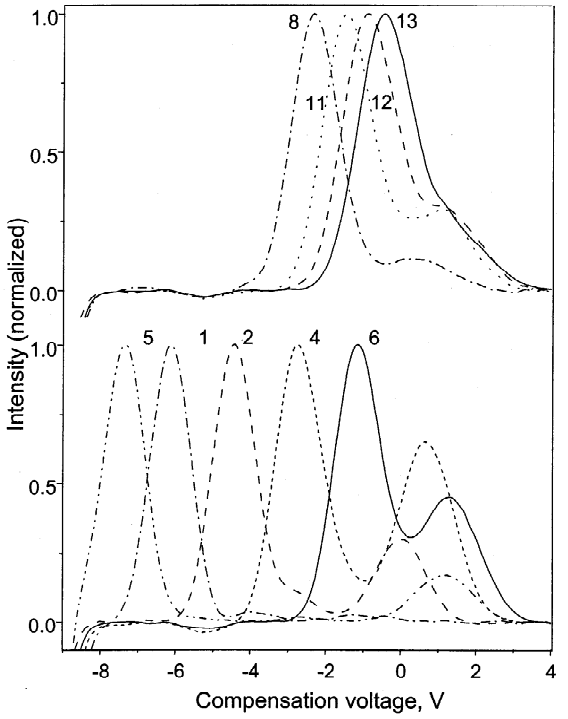

Fig. 7. Plots of detector current versus compensation voltage from RF-IMS scans for esters. Compounds are (1) methyl acetate, (2) ethyl acetate, (4) methyl isobutyrate, (5) *tert*.-butyl acetate, (6) methyl trimethylacetate, (8) *n*-butyl acetate, (11) methyl hexanoate, (12) methyl heptanoate, and (13) methyl octanoate. Numbers for chemicals are the same as those in Fig. 6.

ment ion m/z 57 at ca. 125°C. The location of the peak for *tert*.-butylacetate near that of the reactant ion peak (RIP) (m/z 43 and 57) was consistent with small ions, that is fragment ions. The fragmentation of *tert*.-butylacetate was not observed at temperatures of 50°C in traditional IMS and temperatures of this drift tube were below 50°C. The source for ion decomposition would have to arise from sources other than strictly thermal and could arise from the interaction between the electric field and the protonated monomer of *tert*.-butylacetate. Such interactions with strong RF fields might lead to energetic excitation (i.e. heating) of ions which has been predicted in RF-IMS, though never reported. These results certainly can be understood as ion decomposition through RF heating of the product ions and may suggest that the butylacetates are sensitive indicators of ions heating in atmospheric pressure chemistries.

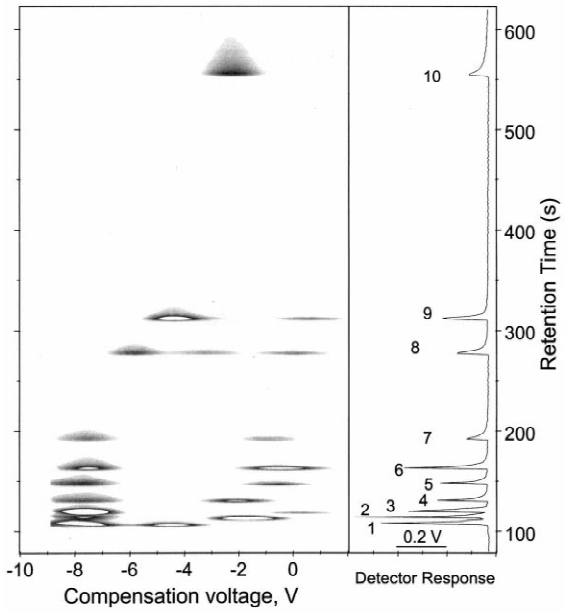

Fig. 8. Results from GC–RF-IMS separation of mixture of alcohols with chromatograms (right frame) and two-dimensional plots of RF-IMS scans (left frame). Peak identities are given in Table 1.

Results from GC–RF-IMS characterization of alcohols is shown in Figs. 8 and 9 and the results were striking in view of previous RF-IMS scans. The chromatography is adequate with only fair peak shape but near baseline resolution throughout the chromatogram. An improved column or perhaps a higher temperature on the detector might improve peak shape. However, the emphasis in this work has been with the detector response and the findings for alcohols was dramatic. For seven of the ten alcohols, regardless of molecular mass or expected size of an MH^+, product ions exhibited an intense peak at -7.6 to -7.3 V_{dc}. These peaks are intense and are accompanied in each instance by another, not as intense, peak appearing at -5 to -0.5 V (see Fig. 9 bottom frame). These second peaks are directly proportional to the first peak meaning that the ions are not related via a clustering equilibrium as currently understood in traditional mobility spectrometry. Alcohols are known to undergo atmospheric pressure chemical ionization fragmentation to small ions that are characteristic of the alcohol family, though these fragmentations have been ob-

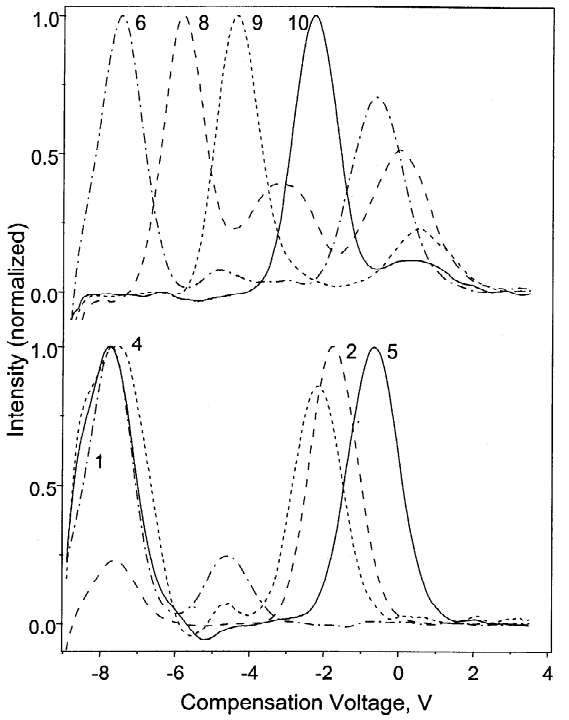

Fig. 9. Plots of detector current versus compensation voltage from RF-IMS scans for alcohols. Compounds are (1) ethanol, (4) 1-propanol, (2) 2-propanol, (5) 2-butanol, (6) 2-methyl-1-propanol, (8) 3-methyl-1-butanol, (9) 4-methyl-2-pentanol, and (10) 2-butoxyethanol. Numbers for chemicals are the same as those in Fig. 8.

served only above 150°C. As with *tert*.-butylacetate, fragmentation of gas phase ions at comparatively low temperatures has not been reported though the patterns for the alcohol scans is suggestive of class wide fragmentation to a specific ion. As with all other results, interpretation here on ion chemistry and identity must be deferred to IMS–MS studies.

4.2. Quantitative studies

The basis for response in this detector is the gas phase chemistry associated with atmospheric pressure chemical ionization mass spectrometry, namely proton transfer reactions between a reservoir of charge and sample neutrals. These reactions are know to provide detection limits in the picogram range and exhibit preferential response toward compounds with strong proton affinities. This analyzer had an ion source that was 1/5th that of conventional IMS drift tubes which are equipped with 10 mCi of ^{63}Ni. Also, the source in this instance (~2 mCi) may have had the effective ionization strength lowered by the fixture used to hold the source in the drift tube. Thus, the detection limits of 0.1–1 ng were anticipated. Actual detection limits were determined as 10–90 pg as shown in Table 1. These should be considered nominal and could be improved by thermostating the drift tube to elevated temperatures and by improving chromatographic performance. Nonetheless, these detection limits match, or better, those for other portable GC detectors. At high masses, the response first became level, i.e. the ion source was saturated, at >100 ng. Above this value, the vapor concentration levels were so high that spectra were distorted through ion–molecule clustering. This caused high uncertainty in quantitative determinations at high nanogram levels and effectively set an upper limit of 10 ng for quantitative usefulness without the addition of servo inlets.

The response curves for aldehydes and esters are shown in Fig. 10 for sample masses of 0.1–5 ng. The plots show linear ranges of ~10 with slight curvature below 0.2 ng. The sensitivity was ca. 4 pA ng^{-1} and differences between relative response of aldehydes and esters were not pronounced and nearly within statistical variation. Differences within the aldehydes were as large as that between aldehydes and esters. The repeatability of peak area was 0.05 pA as shown with the error bar in Fig. 10 resulting in relative repeatability of 2 to ~30% depending upon mass. In contrast, the repeatability of the position of V_{dc} was better than 5% indicating high stability for the electronics and flow controls on the RF-IMS system.

4.3. Application with pheromones and insect attractants

The initial motivation for this work arose from an interest in detecting pheromones on-site in planted fields as part of insect management methods. Two materials that might be present in a field include a non-pheromone mixture known as Mix M. This is a synthetic mixture which is used as an insect attractant resembling grasses. The commercially available pheromone was Grandlure. One interest was to learn if the small detector could provide characteristic

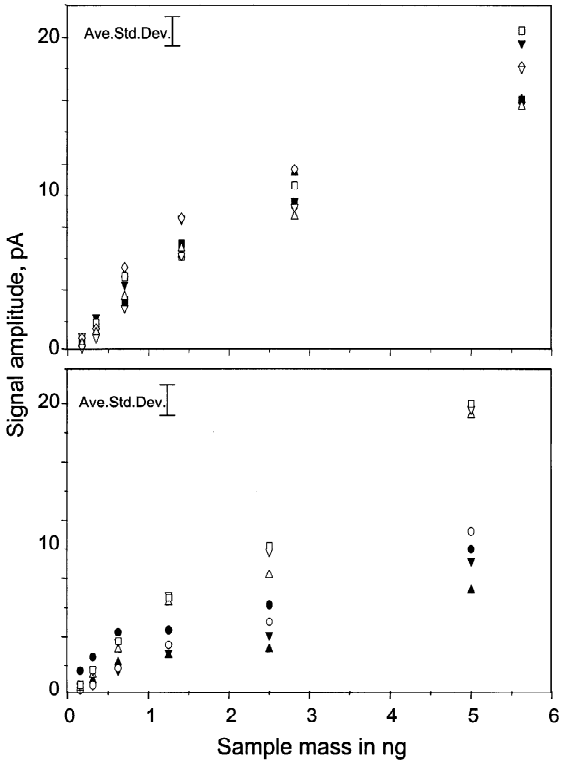

Fig. 10. Calibration curves for selected esters (top frame) and aldehydes (bottom frame). Identities for esters are ■ ethyl acetate, ▲ isopropyl acetate, ▼ methyl isobutyrate, □ *tert*.-butylacetate, ◇ methyl pyruvate, △ methyl isovalerate, and ▽ *n*-butylacetate. Identities for aldehydes are ● 2-methylpropanal, ▲ butanal, ▼ pentanal, ○ hexanal, △ heptanal, ▽ octanal, and □ nonanal.

RF-mobility scans toward the development of on-site gas chromatograph for in-field measurements. Results from GC–RF-IMS characterization of the commercial pheromone, Grandlure, is shown in Fig. 11. Grandlure is a mixture of four components, including a pair of geometric isomers. Four principal components can be seen in the chromatogram. The pair at ~600 s with resolution of 0.6 is comprised of geometric isomers of 3,3-dimethylcylcohexylideneacetaldehyde. The RF-IMS scans showed product ions with compensation voltages of −2 to 0 V_{dc}. The compounds in GrandLure have comparable ion size or mass and cluster in a narrow range of V_{dc} as shown in the 2D plot of Fig. 11 with a narrow band of retention times.

In contrast, the GC–RF-IMS profiles from characterization of the synthetic mixture (Mix M) are

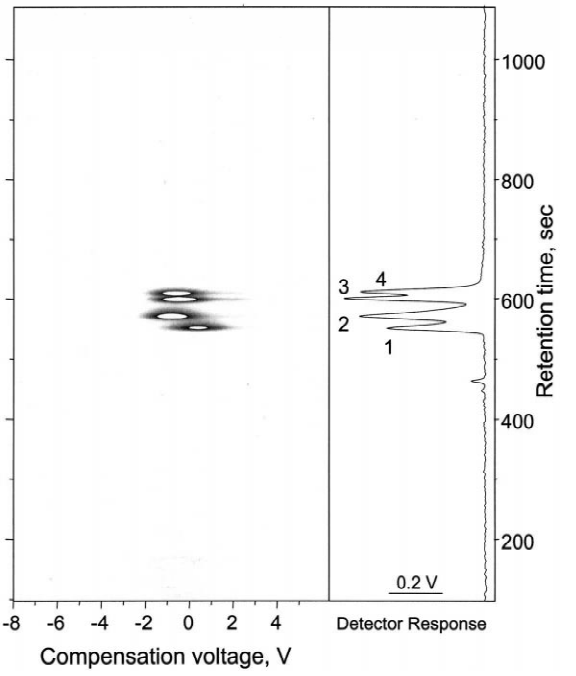

Fig. 11. Results from GC–RF-IMS characterization of Grand Lure. Peaks are (1) ±(*Z*)-2-isopropenyl-1-methylcyclobutylethanol, (2) (*Z*)-3,3-dimethylcylcohexyledeneethanol, (3) (*Z*)-3,3-dimethylcylcohexylideneacetaldehyde, and (4) (*E*)-3,3-dimethylcylcohexylideneacetaldehyde.

easily recognized as distinctive from Grandlure as shown in Fig. 12. Mix M is comprised of five constituents and these can be seen in the chromatogram where five principal constituents elute with retention times between 350 and 750 s. The patterns for peaks in the RF-IMS scans also exhibited a larger range of V_{dc} values than those of Grandlure making a clear and obvious contrast between the two materials. Additional studies with these materials under actual field circumstances are pending the development of ruggedized configurations and such development was deemed plausible in view of the analytical performance of this prototype analyzer.

5. Conclusion

A small gas chromatographic detector was made from an RF-IMS analyzer and was equipped with a β ionization source. The detector provided orthogonal

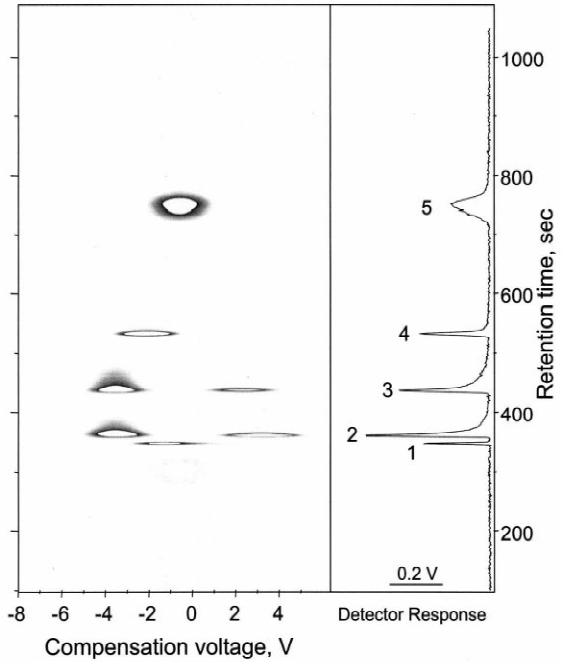

Fig. 12. Results from GC–RF-IMS characterization of Mix M. Peaks are (1) *R*(+)-limonene, (2) phenylacetaldehyde, (3) 2-phenylethanol, (4) methyl salicylate, and (5) methyl 2-methoxybenzoate.

information to that of chromatographic retention and RF-IMS scans were available throughout the GC separation. Several scans were available for each component resolved in the gas chromatograph. Results for alcohols, aldehydes, esters, and ethers demonstrated the breadth of response with distinctive profiles from the ion characterization using the RF-IMS concept. The detector provided repeatable response with standard deviations on peak heights of 10–20% ($n=3$) and a working range from 0.1 to 100 ng. Limits of detection ranged from 10 to 90 pg and these are sufficient for general use as a detector for on-site gas chromatographs. The size, mass and power consumption also favor continued development of this mobility analyzer as a detector for field gas chromatographs. In future studies, a thermostated detector made from glass will be expected to provide improved peak shape in RF-IMS scans and perhaps still better detection limits.

Acknowledgements

Support is gratefully acknowledged from the university cooperation grants from Charles Stark Draper Laboratory (Award No. DL-H-516600) and the Idaho National Environmental Engineering Laboratory, Ion Mobility Spectrometry Partnership Program. Support from project # I.C. (1999–2000) from the Cotton Foundation General Research and Education Program is gratefully acknowledged.

References

[1] R. Annino, J. Chromatogr. A 678 (1994) 279.
[2] R.C.M. Denijs, J. Vandalen, A.L.C. Smit, E.M. Vanloo, J. High Resolut. Chromatogr. 16 (1993) 379.
[3] E.S. Kolesar, R.R. Reston, IEEE Trans. Component Pack. Manuf. Tech. Part B. Adv. Packaging 21 (1998) 324.
[4] J.S. Alvarado, J. Silzer, F. Lemley, M.D. Erickson, Anal. Commun. 34 (1997) 381.
[5] M. vanLieshout, M. vanDeursen, R. Derks, H.G. Janssen, C. Cramers, J. Microcol. Sep. 11 (1999) 155.
[6] M. vanLieshout, M. vanDeursen, R. Derks, H.G. Janssen, C. Cramers, J. High Resolut. Chromatogr. 22 (1999) 119.
[7] J.I. Baumbach, G.A. Eiceman, D. Klockow, S. Sielemann, A.v. Irmer, Int. J. Environ. Anal. Chem. 66 (1997) 225.
[8] M. vanLieshout, M. vanDeursen, R. Derks, H.G. Janssen, C. Cramers, J. High Resolut. Chromatogr. 22 (1999) 116.
[9] V. Jaim, J.B. Phillips, J. Chromatogr. Sci. 33 (1995) 541.
[10] See web site for INFICON at http://www.hapsite.com/
[11] M.J. Cohen, in: A. Zlatkis (Ed.), Chromatography Symposium, Houston, TX, Advances in Chromatography, 1970.
[12] M.A. Baim, H.H. Hill Jr., Anal. Chem. 54 (1982) 38.
[13] S.E. Bell, E. Nazarov, Y.F. Wang, J.E. Rodriguez, G.A. Eiceman, Anal. Chem. 72 (2000) 1192.
[14] E.S. Reese, S.J. Taraszewski, T.F. Limero, J.T. James, Presented at the 8th International Conference on Ion Mobility Spectrometry, Buxton, UK, 8–12 August, 1999.
[15] G.A. Eiceman, Y.-F. Wang, L. Garcia-Gonzalez, C.S. Harden, D.B. Shoff, Anal. Chim. Acta 306 (1995) 21.
[16] A. Mercado, P. Marsden, in: Proceedings of the 3rd International Workshop on Ion Mobility Spectrometry, USA, April, 1995, p. 168.
[17] A.P. Snyder, C.S. Harden, A.H. Brittain, M.G. Kim, N.S. Arnold, H.L.C. Meuzelaar, Anal. Chem. 65 (1993) 299.
[18] A.P. Snyder, C.S. Harden, D.B. Shoff, L. Katzoff, Air Waste Manag. Assoc. 2 (1995) 683.
[19] J.I. Baumbach, D. Berger, J.W. Leonhardt, D. Klockow, Int. J. Environ. Anal. Chem. 52 (1993) 189.
[20] J. Xu, W.B. Whitten, J.M. Ramsey, Presented at the 8th International Workshop on Ion Mobility Spectrometry, Buxton, UK, 8–12 August, 1999.

[21] R.A. Miller, G.A. Eiceman, E.G. Nazarov, Sensors Actuators B Chem. 67 (2000) 300.
[22] I.A. Buryakov, E.V. Krylov, E.G. Nazarov, U.Kh. Rasulev, Int. J. Mass Spectrom. Ion Proc. 128 (1993) 143.
[23] R.W. Purves, R. Guevremont, S. Day, C.W. Pipich, M.S. Matyjaszczyk, Rev. Sci. Instrum. 69 (1998) 4094.
[24] B. Ells, K. Froese, S.E. Hrudey, R.W. Purves, R. Guevremont, D.A. Barnett, Rapid Commun. Mass Spectrom. 14 (2000) 1538.
[25] R.W. Purves, R. Guevremont, Anal. Chem. 71 (1999) 2346.
[26] R. Guevremont, R.W. Purves, J. Am. Soc. Mass Spectrom. 10 (1999) 492.
[27] R. Guevremont, R.W. Purves, D.A. Barnett, L. Ding, Int. J. Mass Spectrom. Ion Proc. 193 (1999) 45.
[28] H.E. Revercomb, E.A. Mason, Anal. Chem. 47 (1975) 970.
[29] G.A. Eiceman, E.G. Nazarov, B. Tadjikov, R.A. Miller, Field Anal. Chem. Technol. 4 (2000) 297.